Amino-attapulgite/mesoporous silica composite films generated by electro-assisted self-assembly for the voltammetric determination of diclofenac

Sherman L.Z. Jiokeng, Ignas Tonle, Alain Walcarius

Amino-Attapulgite/mesoporous silica composite films generated by electro-assisted self-assembly for the voltammetric determination of diclofenac

Sherman L. Z. Jiokeng,[a,b] Ignas K. Tonle[a] and Alain Walcarius[b]

[a]*Electrochemistry and Chemistry of Materials, Department of Chemistry, University of Dschang, P.O. Box 67 Dschang, Cameroon*
[b]*Laboratoire de Chimie Physique et Microbiologie pour les Matériaux et l'Environnement (LCPME), UMR 7564 CNRS – Université de Lorraine; 405, rue de Vandœuvre, 54600 Villers-lès-Nancy, France*

Abstract

Diclofenac (DCF) is a common anti-inflammatory drug. In this work, we have developed two new modified electrodes based on attapulgite clay mineral for the determination of DCF. The first one is made of an amino-functionalized attapulgite modified glassy carbon electrode (GCE/Amino-AT) issued from the grafting of attapulgite particles with [3-(2-aminoethylamino)propyl]trimethoxysilane. Voltammetric data indicate slightly easier oxidation of DCF on such modified electrode (irreversible anodic peak at +0.750 V *vs.* Ag/AgCl *i.e.,* about 85 mV lower than on bare GCE), and pH-dependent response resulting from interactions between the probe and the electrode material. The second one is an amino-attapulgite–mesoporous silica composite film generated by electro-assisted self-assembly of a surfactant-templated silica layer entrapping the amino-functionalized attapulgite particles on GCE pretreated by electrografting of [3-aminopropyl]triethoxysilane (GCE/APTES-Amino-AT-Silica), which was designed in order to avoid the loss of clay particles in solution over prolonged use of the modified electrode. After characterization of the film morphology, composition and permeability, respectively by scanning electron microscopy (SEM), energy-dispersive X-ray spectroscopy (EDX) and cyclic voltammetry (CV), the modified electrodes were applied to the detection of DCF by square wave voltammetry (SWV). Both electrodes gave rise to SWV peak currents varying linearly with DCF concentration in the range of 0.3 – 20 μM (in phosphate buffer at pH 5.7). The detection limits were 0.204 μM on GCE/Amino-AT and 0.053 μM on GCE/APTES-Amino-AT-Silica. The proposed method was successfully applied to the determination of DCF in pharmaceuticals and water samples.

Keywords: Diclofenac, attapulgite clay, mesoporous silica, film electrode, voltammetric sensor.

1. Introduction

Nonsteroidal anti-inflammatory drugs (NSAIDs) belong to a therapeutic class of drugs useful in the treatment of pains and rheumatoid arthritis [1,2]. Pharmaceuticals become more and more present in the environment as new emerging pollutants. They are thus currently being considered ubiquitous contaminants in waters, soils and sediments, and can be prejudicial to both aquatic biota [3] and human health [4]. With increasing regulatory pressures on the pharmaceutical industry, there is a growing need for robust sensors that could allow rapid and reliable determinations, and this is particularly the case in quality control analysis. One class of pharmaceuticals frequently found in water concerns the anti-inflammatory drugs, among which diclofenac (DCF, [o-(2,6- dichloroanilino]phenyl] acetate) can be considered as a representative-model. DCF is a non-steroidal, anti-inflammatory drug with analgesic and antipyretic properties, extensively used to relieve the symptoms of arthritis (i.e., inflammation, swelling, stiffness and joint pains) [5,6].

DCF is likely to increase the blood pressure in patients with Shy-Drager syndrome and diabetes mellitus. In case of long-term use, it may also cause life-threatening heart or circulation problems such as heart attack and stroke, or serious effects on the stomach or intestines (such as bleeding or perforation) [7]. Therefore, it is vital to develop simple, fast, selective and cost-effective methods for the determination of trace amounts of DCF in pharmaceuticals and biological samples to prevent their potential human health and environment impacts. The quantification methods of DCF include mostly separation techniques such as gas chromatography-mass spectrometry [8,9], liquid chromatography [10-13], high-performance liquid chromatography (HPLC) [14-16], as well as spectrophotometry [17-20] and spectrofluorometry [17,18]. Most of them are time consuming, expensive, and often need complicated preconcentration as well as derivatization. By contrast, electrochemical techniques are rather fast and simple, and they can be implemented as portable and low cost devices. Thus, some electrochemical methods have been developed for the sensitive detection of DCF [21-22]. Various nanomaterials have been used as electrode modifier for the electroanalytical determination of DCF in pharmaceutical formulations and biological fluids, including carbon nanotubes [7,23], metal nanoparticles [24,25] and other composites materials [22,23,26]. The interaction between the target and these materials mainly relies on the electrocatalytic activity of the latter.

The interest of nanomaterials in electroanalysis has prompted the development of organoclay modified electrodes, which are nowadays investigated as sensors [27] or biosensors [28] for pharmaceuticals. Organoclays are composite materials obtained by functionalizing pristine

clay materials with selected organic compounds. They are commonly prepared by one of the following processes: intercalation, ion exchange, pillaring or surface grafting [29-31]. As well, silica-based mesoporous materials are attractive electrode modifiers due to their mechanically-stable structure at the nanoscale (with long-range order, controlled pore size, high surface area and large adsorption capabilities) [32-37]. These materials can be prepared in the form of thin films [38], or as inorganic-organic hybrids via appropriate surface modification [39], extending thereby their properties. Various strategies have been developed to prepare nanostructured silica coatings onto electrode surfaces [40], and an attractive configuration is that made of hexagonally packed mesochannels aligned normal to the solid support [37], as it ensures fast mass transport processes from the external solution. A versatile way to get such oriented mesoporous silica films is the electrochemically assisted self-assembly (EASA) method [41,42]. EASA is based on the use of cetyltrimethylammonium bromide (CTAB) as the surfactant template to generate materials with pore diameter ranging from 2 to 3 nm. In this method, the electrode is immersed into a prehydrolyzed sol formed by tetraethoxysilane (TEOS) and CTAB in moderately acidic medium (pH 3), and a suitable reductive potential is applied to generate hydroxyl ions locally at the electrode/solution interface. The local pH increase contributes to catalyze the condensation of precursors [43-45] and, in the same time, the formation of surfactant hemimicelles, which orients the growth of the mesoporous silica film in a direction perpendicular to the electrode surface by self-assembly [41,42]. EASA method can be also applied to prepare functionalized mesoporous silica layers, with great promise for the elaboration of sensitive electroanalytical devices [46]. In addition, sol-gel electrogeneration is compatible with the encapsulation of biomolecules to build bioelectrocatalytic devices [47,48], or can be used to generate clay-mesoporous silica composite films [49].

In this work, we have investigated the interest of amine-functionalized attapulgite clay as electrode modifier for diclofenac determination. We have also used the EASA method to generate amino-attapulgite-mesoporous silica composite films onto glassy carbon electrodes (pretreated by electrografting of 3-aminopropyltriethoxysilane, APTES, to ensure good adhesion of silica [50]), which are likely to be more mechanically stable than those elaborated from only clay particles. After characterization of their physico-chemical features and permeability properties using selected redox probes (cationic, neutral and anionic), we demonstrated that this composite electrode can be used for preconcentration and sensitive detection of DCF in water and pharmaceutical samples. To the best of our knowledge, no electrochemical sensor of this type has been reported so far.

2. Experimental section

2.1. Chemicals and reagents

All chemicals and reagents (analytical grade) were used without further purification. [3-Aminopropyl]triethoxysilane (APTES, 99%), tetrabutylammonium tetrafluoroborate (Bu_4NBF_4, 99%), and acetonitrile (99.9%) used for the electrografting of APTES onto the glassy carbon surface were purchased from Sigma-Aldrich. Tetraethoxysilane (TEOS, 98%, Alfa Aesar) and cetyltrimethylammonium bromide (CTAB, 99%, Acros) were used for the synthesis of mesoporous silica film, from solutions prepared with ethanol (95-96% Merck), $NaNO_3$ (99%, Fluka), and HCl (Riedel de Haen, 1 M solution). Hexaammineruthenium(III) chloride ($Ru(NH_3)_6Cl_3$, 98%, Aldrich), ferrocene dimethanol ($Fc(MeOH)_2$, Alfa Aesar) and potassium hexacyanoferrate(III) ($K_3Fe(CN)_6$, Fluka) served as redox probes for permeability characterization of the film modified electrodes. Diclofenac sodium ($C_{14}H_{10}Cl_2NNaO_2$, 98%, Sigma-Aldrich), and various electrolytes such as NaCl (99 %, Prolabo) or phosphate buffer solution (PB, 0.1 M, pH 5.6), as prepared from $Na_2HPO_4.2H_2O$ (98%, Fluka), and KH_2PO_4 (99%, Normapur), were used for square wave voltammetry analyses. High-purity water (18.2 MΩ cm) was obtained from a Purelab Option-Q from ELGA and used for all experiments. Real samples (collected in Nancy, France) were made of mineral water, tap water and natural water from the strengbach watershed (referred as SB water). They were filtered using Durapore Membrane filters (HVLP 0.45µm, Millipore) and then stored at 4°C. Crude attapulgite (PFl-1 sample) was obtained from the Source Clay Minerals Repository (Purdue University, West Lafayette, USA). The ideal molecular formula of attapilgite is $Mg_5Si_8O_{20}(HO)_2(OH_2)_4{\cdot}4H_2O$. The mineral possesses surface reactive hydroxyl (-OH) groups and exchangeable cations [51-53]. Its surface area ranges from 125 to 195 m^2/g [54] and it has a good mechanical strength [55]. In this work, a nanohybrid material was prepared by modifying the surface of attapulgite (AT) with grafting an amine terminated organosilane, namely ([3-(2-Aminoethylamino)propyl]trimethoxysilane, AEP-TMS, Aldrich, ≥ 98%), according to a previously published procedure [56,57]. The modified attapulgite (referred as Amino-AT) was used to build an electrochemical sensing device for DCF quantification.

2.2. Preparation of clay films and amino-attapulgite/mesoporous silica films on the GCE

Glassy carbon electrodes (GCE, surface area: 0.071 cm^2) were polished using alumina pastes of different particle sizes (5, 1 and 0.5 µm), then treated in 1:1 ethanol-water solution and sonicated for 10 min for removing any residual alumina particles. Thin film working electrodes were prepared as follow: 6 µL of either Amino-AT or AT dispersions (5 mg mL^{-1})

were drop-coated onto the top of the GCE, which was dried at 50°C for 10 min in an oven. Throughout the text, the modified electrodes are referred to as "GCE/AT" and "GCE/Amino-AT", respectively for GCE modified by pristine AT or Amino-AT; the optimal amount of AT or Amino-AT being 30 µg on the electrode surface.

Clay-mesoporous silica composite films on electrodes were prepared in two successive steps. The first one involved the electrografting of APTES onto GCE via a known procedure in which aliphatic amines are electrochemically oxidized on the electrode surface [50,58]. This was performed by dipping the electrode into a mixture of 1 mM APTES and 0.1 M Bu_4NBF_4 in acetonitrile and by scanning potentials in the +0.7 and +2.0 V range using cyclic voltammetry (scan rate: 100 mV s^{-1}). Upon cycling, the obtained electrodes were rinsed with ethanol. An Amino-AT film (containing 30 µg of Amino-AT) was then formed by drop-coating onto the APTES grafted GCE, as previously reported [56]. Finally, EASA was applied to generate a mesoporous silica film around the Amino-AT particles on GCE (the same electrodeposition protocol was used to modify a clay-free electrode for comparison purposes) [41,42,50]. The sol used was prepared by mixing ethanol and aqueous $NaNO_3$ (0.1 M) in a 1:1 v/v ratio. TEOS and CTAB were then added to this solution according to their previously optimized concentrations (respectively 100 and 32 mM) [42]. Upon adjusting the sol pH to 3 with added HCl, sol hydrolysis was performed at room temperature, under stirring for 2.5 h. Film electrodeposition was achieved after immersion of the electrodes in this sol solution, to which a current density of -0.74 mA.cm^{-2} was applied for 30 s (a silver wire and a Pt wire were used as a pseudo-reference electrode and counter electrode, respectively). To ensure good cross-linking of the silica network, the electrodes were dried overnight at 130 °C. The template was removed as previously described by using 0.1 M HCl in ethanol [46]. The resulting composite films electrodes were denoted "GCE/APTES-Silica" (sample without clay) and "GCE/APTES-Amino-AT-Silica" (sample with amino-functionalized attapulgite).

2.3. Instrumentation and experimental procedures

All electrochemical experiments and galvanostatic depositions were carried out respectively with a µ-Autolab potentiostat and a PGSTAT 100 apparatus from Ecochemie (Metrohm, Switzerland). For electrochemical experiments (cyclic and square wave voltammetry), a conventional three electrode cell configuration was employed. The working electrodes were the film modified GCEs, while an Ag/AgCl/KCl 3 M reference electrode (Metrohm, Switzerland) and a platinum wire counter electrode completed the system. APTES electrografting was carried out with an EMStat2 potentiostat (PalmSens, The Netherlands),

using a silver wire as a pseudo reference and a platinum wire as counter electrode. Cyclic voltammetry was performed in solutions containing 0.5 mM redox probes (in 0.1 M $NaNO_3$). It was used to characterize in a qualitative way the rate and effectiveness of accumulation/rejection processes at the film electrodes investigated here. Conditions for square wave voltammetry measurements were the following: 5 s equilibration time, 4 mV potential step, 20 mV amplitude, and 25 Hz frequency. The morphology of modified GCEs were investigated by scanning electron microscopy (SEM) along with energy-dispersive X-ray spectroscopy (EDX) using a JEOL JCM-6000 apparatus (acceleration voltage of 15 kV).

The pH corresponding to the point of zero charge pH_{pzc} of Amino-AT was measured by the so-called pH drift method [59]. To this end, 4 mL of 0.1 M NaCl solution was placed in a vessel, and its pH was adjusted to values ranging between 2 and 12, by adding either HCl or NaOH; then 5 mg of Amino-AT were added to the solution in the vessel which was sealed. The final pH, reached after 48 h under stirring, was measured and plotted against the initial pH. The pH at which the curve crosses the graph $pH_{(final)}$=$pH_{(initial)}$ was taken as the pH_{pzc} of the Amino-AT.

3. Results and discussion

3.1. Preliminary voltammetric studies on binder-free attapulgite (AT) modified electrodes

Figure 1 illustrates typical cyclic voltammograms recorded in 100 µM DCF using bare GCE and GCE modified with attapulgite (AT) and AEP-TMS-grafted attapulgite (Amino-AT).

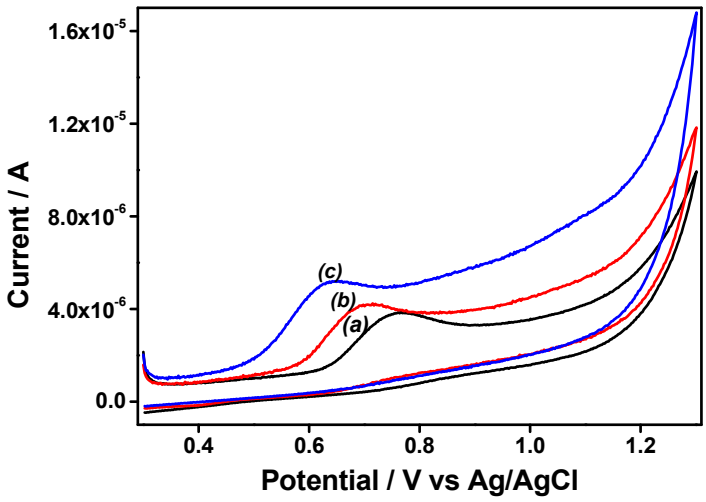

Fig. 1. Cyclic voltammograms of 100 µM DCF at the GCE *(a, black)*, GCE/AT *(b, red)* and GCE/Amino-AT *(c, blue)* in 0.1 M NaCl pH 6. The scan rate was 50 $mV \cdot s^{-1}$.

DCF is irreversibly oxidized on the three electrodes, but peak currents were found to increase when passing from GCE to GCE/AT and to GCE/Amino-AT. At the same time, peak potentials were shifted towards less anodic values: from +0.745 V on bare GCE to +0.660 V on GCE/AT and +0.615 V on GCE/Amino-AT. This indicates an ability of AT, and especially Amino-AT, to induce effective enhancement of the DCF oxidation signal and improved electron transfer rates, suggesting the existence of both accumulation and electrocatalytic effects originating from the grafted material towards the detection of DCF. Similar variations were observed at lower DCF concentrations and using square wave voltammetry (SWV), but actually the responses (i.e., peak potentials and peak currents) were strongly pH-dependent (Fig. 2A&B) and this was attributed to the acid-base properties of DCF, the surface charge of AT and Amino-AT, as well as the oxidation mechanism of DCF, as discussed hereafter. Fig. 2A shows that the oxidation peak potentials of DCF on GCE (curve 1), GCE/AT (curve 2) and GCE/Amino-AT (curve 3) shifted negatively with increasing the solution pH, indicating that protons are involved in the reaction process at the electrode surface. The linear regression equations were Ep = -0.049pH + 0.995 (R = -0.994), Ep = -0.055pH + 0.949 (R = -0.994) and Ep = -0.056pH + 0.986 (R = -0.992), respectively on GCE, GCE/AT and GCE/Amino-AT, demonstrating that equal number of electrons and protons are involved in the oxidation of DCF. According to previously obtained data, it can be concluded that DCF oxidizes in aqueous medium by losing two electrons and two protons to give 5-hydroxy derivative (see scheme S1 in Supplementary Material) [60-62]. The variations of peak currents with pH are plotted in Fig. 2B. The oxidation of DCF occurs from its protonated form so that larger peak currents were observed on bare GCE (see curve 1 in Fig. 2B) at pH values lower than the pKa value (3.8) of DCF [63]. Almost the same variation was observed for GCE modified with AT (see curve 2 in Fig. 2B), except that slightly larger response was obtained due to some accumulation of DCF on the AT surface, most probably via hydrogen bonding to the surface hydroxyl groups of the clay. In acidic medium, electrostatic interactions between protonated DCF and the negatively charged AT surface (the point of zero charge (pH_{pzc}) of attapulgite was estimated to about 6 by potentiometric titration experiment [64]) are also possible. The behavior of GCE/amino-AT was totally different, showing poor response at pH lower than 3 and significant increase in peak currents at pH larger than 4 (see curve 3 in Fig. 2B). This increase is explained by the effective accumulation of negatively charged DCF (deprotonated at pH above 3.8) and positively charged Amino-AT surface (amino groups are protonated over the whole pH range of Fig. 2B). The point of zero charge (pH_{pzc}) of Amino-AT was evaluated to 8.9 by the so-called pH drift method (see Fig. 2C). Amino-AT is thus always in

its protonated form in the whole pH range 1-7 considered here (pH < pH_{pzc}). Between pH 5 & 7, the SWV current response of GCE/Amino-AT was almost one order of magnitude larger than those obtained at GCE and GCE/AT. For further experiments with GCE/amino-AT, the accumulation/detection of DCF was performed at pH 5.7, an optimal value (Fig. 2B) corresponding also to that of unbuffered aqueous medium.

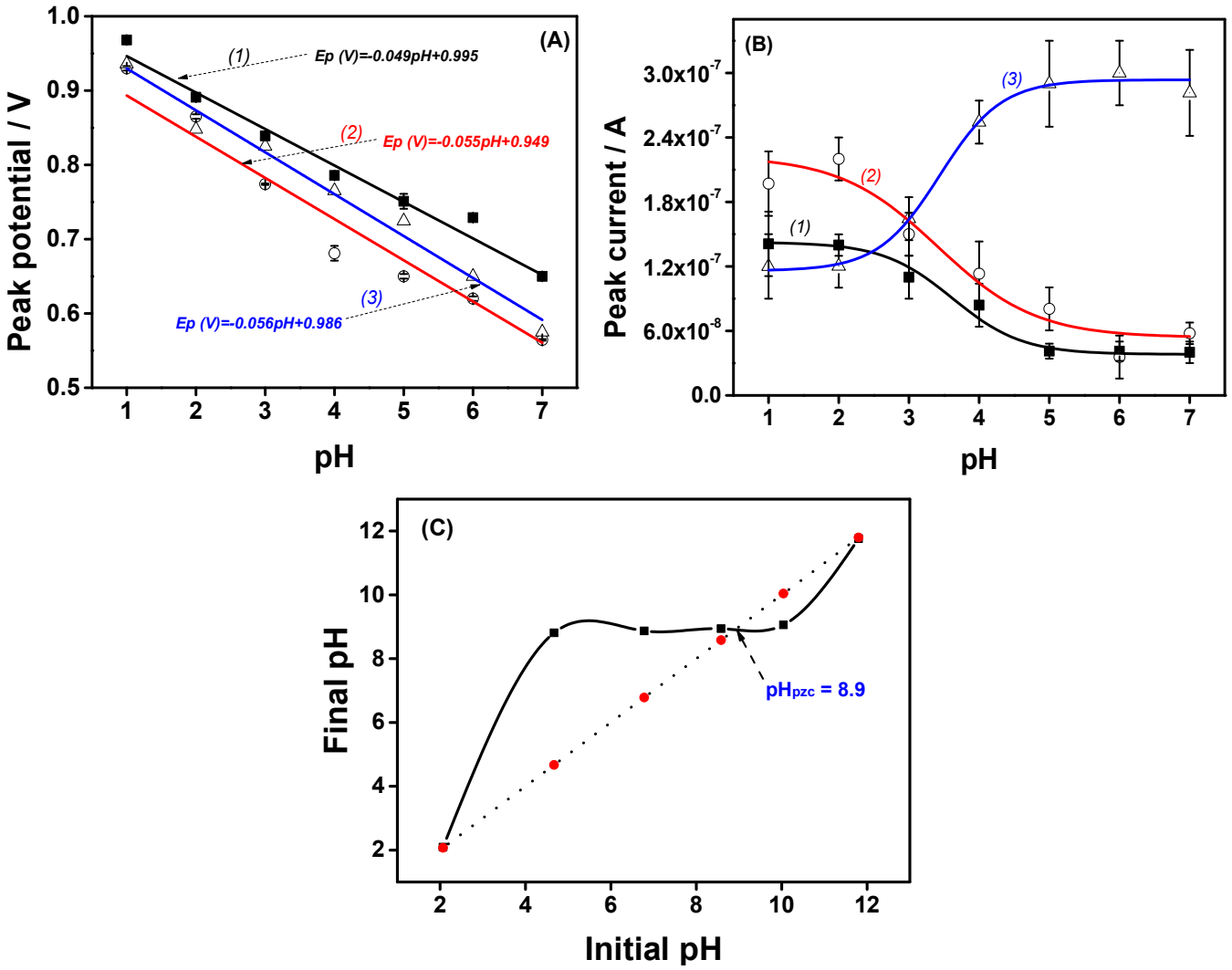

Fig. 2. Influence of pH on (A) the peak potential and (B) SWV Response (peak current) recorded in triplicate for the electrooxidation of 1 µM DCF at GCE *(1, black)*, GCE/AT *(2, red)* and GCE/Amino-AT *(3, blue)*. Accumulation time: 3 min in 0.1 M NaCl, with pH adjusted by adding HCl or NaOH. (C) pH drift method to obtain the pHpzc of Amino-AT.

The SWV response of DCF at an Amino-AT modified GCE was also influenced by the ionic strength (as investigated from solutions containing 30 to 100 mM NaCl, see Fig. S1 in Supplementary Material). Peak currents were first found to increase, reaching a maximum at 0.10 M of NaCl, and then decreasing continuously for larger the ionic strength values. Such slow decrease can be explained by somewhat impeded accumulation of the negatively charged DCF due to competition with the electrolyte anion (Cl^-) for the binding sites of protonated Amino-AT, whereas lower intensities observed in more diluted solutions could be due to increased solution resistance. Finally, the possible effect of the nature of the electrolyte anion on the GCE/Amino-AT electrode response was also investigated using various electrolyte anions (Cl^-, NO_3^-, SO_4^{2-} and $H_2PO_4^-$). No noticeable difference was observed, except for the phosphate medium. In that case, however, it was more related to a buffer effect, maintaining constant the fixed pH (*i.e.*, at 5.7) better than the non-buffered NaCl solution for which DCF oxidation might induce some local pH increase at the electrode surface due to the associated consumption of protons (scheme 1). Such event would contribute to less protonated amino groups and therefore lesser preconcentration ability of the organoclay and smaller peak current intensity (compare curves (a) and (c) in Fig. S2 in Supplementary Material). A control experiment supporting this hypothesis/explanation is the more intense response observed when intentionally protonating all the amino groups of Amino-AT by HCl prior to SWV analysis in NaCl solution (see curve (b) in Fig. S2 in Supplementary Material).
In conclusion, DCF detection is the most sensitive when using GCE/Amino-AT electrode and the best conditions for detection are a phosphate buffer medium at pH 5.7 and ionic strength of 0.1 M. These conditions will be used afterwards.

3.2. Preparation and physico-chemical characterization of Amino-AT-silica composite films

The above results show that an GCE/Amino-AT electrode seems promising for the electrochemical sensing of DCF. However, the simple deposition of Amino-AT particles onto the GCE surface may lead to an organoclay film of poor mechanical stability (loss of clay particles upon prolonged use) so that we have proposed to electrogenerate a silica deposit around the clay particles in order to improve their durable adhesion to the GCE (as for montmorillonite clays [49]). To avoid any unwanted restricted access of the analyte to the electrode surface, a surfactant-templated silica film was generated and the surfactant molecules were removed afterwards to liberate the porosity.

3.2.1. Characterization by Scanning Electron Microscopy (SEM) and Energy-Dispersive X-ray spectroscopy (EDX)

A random distribution of solid particles onto a solid electrode is expected to occur when it has been modified simply by depositing raw clay or organoclay samples [65]. This fact was explored by using SEM analysis. Typical SEM micrographs of Amino-AT particles deposited by drop-coating onto the surface of GCE are shown on Figure 3, as respectively obtained before (Fig. 3a_1) and after (Fig. 3a_2) use in a stirred solution for 30 min.

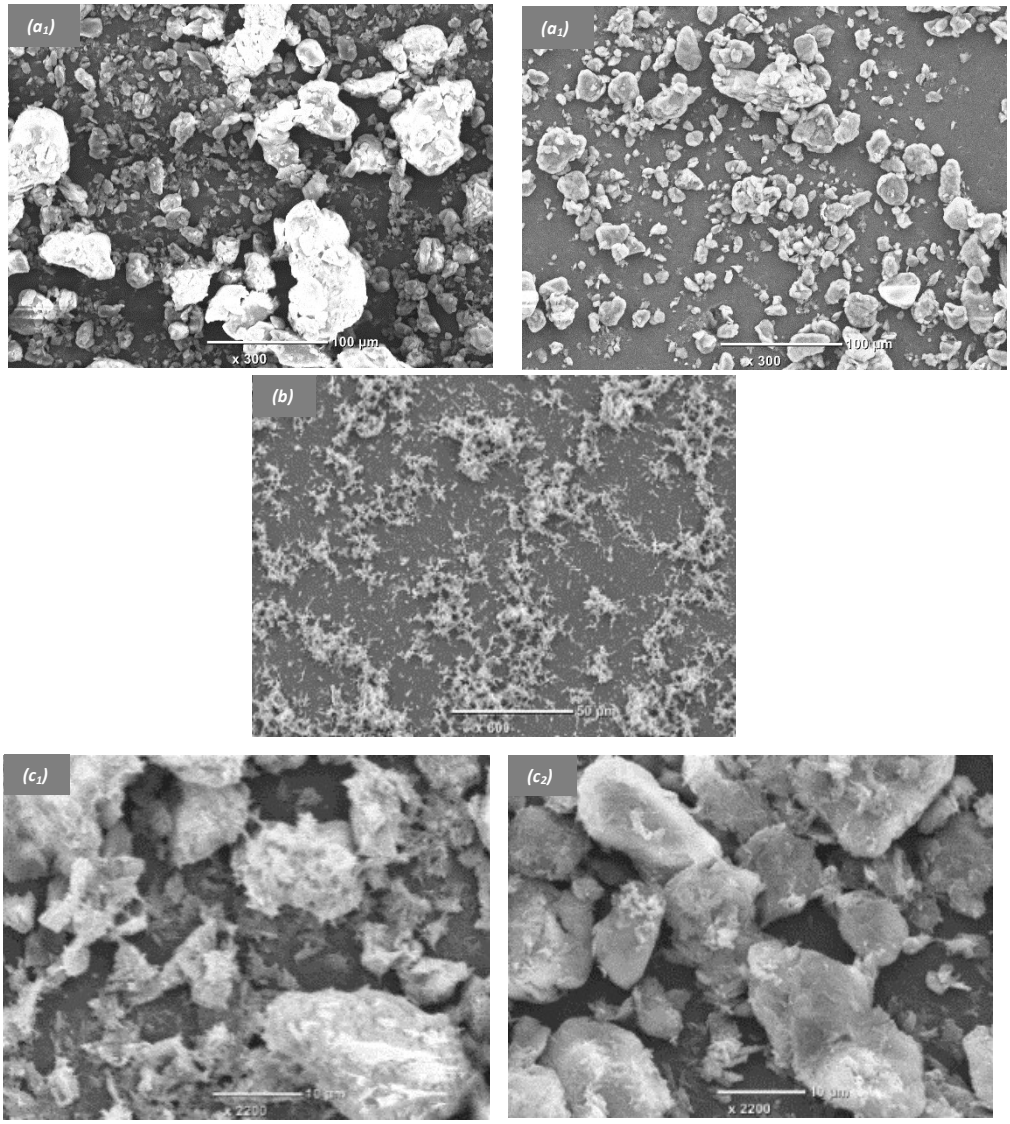

Fig. 3. SEM micrographs of GCE covered with various films: Amino-AT particles before (a_1) and after 30 min use in solution (a_2), mesoporous silica (b), and Amino-AT-Silica before (c_1) and after 30 min use in solution (c_2).

The surface of GCE/amino-AT is heterogeneous, made of small particles of about 10 µm size and bigger aggregates of more than 50 µm (Fig. $3a_1$), but the most important feature is that the quantity of Amino-AT onto the electrode surface decreases after prolonged use in the electrochemical cell (Fig. $3a_2$). This is most probably due to the poor adhesion of Amino-AT particles to the electrode surface. To improve the mechanical stability of the clay film on GCE, we propose to generate a mesoporous silica film by electro-assisted deposition (similarly as in [41,42]), with the hope that the silica coating will entrap the clay particles thus improving their durable attachment to the electrode surface. Because silica is not expected to bind to the carbon surface, a "molecular glue" was first generated by electrografting APTES onto the GCE surface prior to deposition of the mesoporous silica film by EASA [50]; in that case, a uniform coating is obtained, yet with some silica particles on the top, in agreement to previously reported observations [41,42,46,50] (see Fig. 3b for a mesoporous silica film deposited onto bare GCE). EASA was then applied to the GCE/Amino-AT electrode. From what one knows from literature about EASA applied to an electrode covered with an assembly of microparticles (i.e., polystyrene beads [66]), two successive steps are likely to occurs: a fast starting deposition around the solid particles (surface gelification is often faster than bulk one [67]), and a subsequent filling of the free interstitial spaces. It seems to be also the case here, with a mesoporous silica film electrogenerated around the Amino-AT particles and onto the GCE surface, which is mostly visible via the presence of the silica beads everywhere (see SEM micrograph on Fig. $3c_1$). More importantly the so-obtained Amino-AT-mesoporous silica composite films were mechanically stable after prolonged use in solution (no noticeable loss of clay particles, see Fig. $3c_2$), confirming that both electrografted APTES and electrogenerated silica contribute to improve the adhesion of the amino-AT particles to the GCE surface. The GCE/APTES-Amino-AT-Silica film was also examined by EDX using the SEM microscope by focusing either on clay particles or on electrode surfaces free of clay (see Fig. S3 in Supplementary Material). The EDX spectrum showed that the modified electrode in spot (001) (*i.e.*, with clay particle, see Fig. S3a) contained C, Na, N, O, Mg, Al and Si elements in relation to the presence of both Amino-AT and silica onto the electrode surface. In spot (002) (*i.e.*, without clay particle, see Fig. S3b) only C, O and Si elements are evidenced, confirming the presence of a silica film also onto the clay-free electrode surface. To further point out that Amino-AT film is mechanical stable on GCE/APTES-Amino-AT-Silica after electrogeneration of mesoporous silica film, GCE/APTES-Amino-AT-Silica films before and after prolonged uses (*ca.* 30 min) were also examined by EDX using the SEM microscope by focusing on full SEM images surface (see Fig. S4 in Supplementary Material).

The EDX spectrum of the electrode before (Fig. S4a) and after uses (Fig. S4b) showed that the mass percentage of O, Mg and Si elements are roughly the same, confirming the stability of electrode. Also, during the preparation of GCE/APTES-Amino-AT-Silica, it was necessary to extract the surfactant from the mesoporous silica using 0.1 M HCl in ethanol solution under moderately stirring for 2 hours while the GCE electrode was not subjected to stirring before use. Therefore, it can be reasonably admitted that the mesoporous silica allowed stabilizing Amino-AT particulate film not only during the detection phase but also during the development of the sensor. These results clearly confirm the presence of the mesoporous silica films on the modified electrode surface, acting as a stabilization coating for maintaining Amino-AT particles durably onto the GCE surface.

3.2.2. Permeability properties of the various films evaluated by cyclic voltammetry (CV)

The reactivity of an electrode coated with a film/material strongly depends on its permeability properties. This can be examined using redox probes in solution [68]. Cyclic voltammetry was thus applied to characterize six electrodes (bare GCE, GCE/APTES-Silica before and after surfactant removal, GCE/APTES-Amino-AT-Silica before and after surfactant removal, and GCE/Amino-AT), using three relevant redox probes ($[Fe(CN)_6]^{3-}$, $Fc(MeOH)_2$ and $[Ru(NH_3)_6]^{3+}$), and the results are summarized in Fig. 4. The three probes were first analyzed at a bare GCE and gave the expected well defined reversible CV signals (see curves (1) in parts A-C of Fig. 4). When the APTES pre-coated GCE was covered by a thin mesoporous silica film, before template removal, the response to the ionic probes ($[Fe(CN)_6]^{3-}$ and $[Ru(NH_3)_6]^{3+}$) was suppressed (see curves (2) in parts A&C of Fig. 4) because the surfactant-containing silica film acts as a barrier to both negatively and positively charged species [69]. This also proves the formation of a continuous film of silica on the whole electrode surface without cracking. By contrast, a pair of well-defined current peaks was observed for $Fc(MeOH)_2$ (see curve (2) in parts B of Fig. 4) because such neutral probe can permeate the CTAB surfactant phase and be detected on the underlying electrode surface [41]. After surfactant removal, the mesoporous silica film modified electrodes displayed current responses for all three probes but with an obvious charge permselectivity (small response for $[Fe(CN)_6]^{3-}$ and large signals for $[Ru(NH_3)_6]^{3+}$ and $Fc(MeOH)_2$, see curves (3) in parts A-C of Fig. 4). This is due to the negatively charged internal surface of ultrasmall channels (arising from the presence of silanolate groups), generating thereby some charge permselectivity [68]. All these results agree well with those reported previously [41,69].

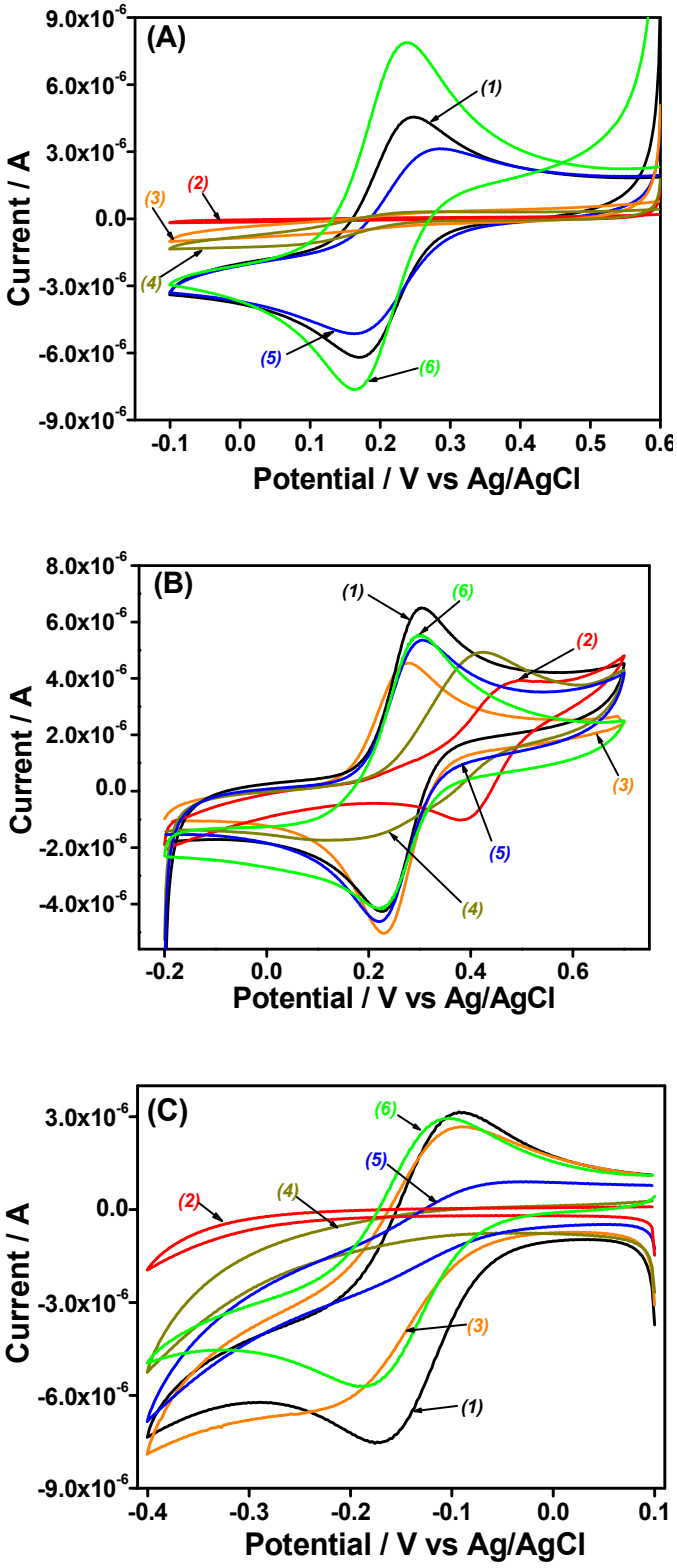

Fig. 4. Cyclic voltammograms recorded in 0.1 M $NaNO_3$ containing (A) 0.5 mM $[Fe(CN)_6]^{3-}$, (B) 0.5 mM $Fc(MeOH)_2$ and (C) 0.5 mM $[Ru(NH_3)_6]^{3+}$, using various electrodes: (1) bare GCE; (2,3) GCE/APTES-Silica before (2) and after surfactant removal (3); (4,5) GCE/APTES-Amino-AT-Silica before (4) and after surfactant removal (5); (6) GCE/Amino-AT. The potential scan rate was 50 mV s^{-1} in all cases.

Now, let's consider the amino-attapulgite–mesoporous silica composite film modified GCE. Before surfactant extraction, the results were almost the same as those obtained for the clay-free mesoporous silica film modified GCE, except that little permeability started to occur due to possible diffusion of the probes through clay aggregates incompletely covered with silica (see curves (4) in parts A-C of Fig. 4). After surfactant removal, the clay-silica composite film exhibited a dramatically different behavior as the mesoporous silica film alone in the presence of the ionic probes ($[Fe(CN)_6]^{3-}$ and $[Ru(NH_3)_6]^{3+}$) whereas almost no difference was observed for the neutral $Fc(MeOH)_2$ species (compare curves (5) and (3) in parts A-C of Fig. 4). This is clearly due to electrostatic interactions induced by the Amino-AT particles present onto the electrode surface, which enable effective permeation to the negatively-charged $[Fe(CN)_6]^{3-}$ ions and consequently large peak currents (see curve (5) in Fig. 4A) thanks to electrostatic attractions from the protonated Amino-AT material, while repelling the cationic probe (see curve (5) in Fig. 4C showing the poor response to $[Ru(NH_3)_6]^{3+}$). The effective permeation to the negatively-charged $[Fe(CN)_6]^{3-}$ ions was even more pronounced when using a silica-free Amino-AT film electrode (GCE/Amino-AT), and even larger peak currents were observed (compare curves (6) and (5) in Fig. 4A), because of the absence of the mesoporous silica "barrier" likely to repel anions. On the other hand, the blocking effect towards $[Ru(NH_3)_6]^{3+}$ cations was no more observed in the absence of the silica binder (compare curves (6) and (5) in Fig. 4C) as this probe was likely to reach the electrode surface by diffusion across film (i.e., between clay particles) when using the GCE/Amino-AT electrode. Again, no noticeable difference between GCE/Amino-AT and GCE/APTES-Amino-AT-Silica when using the neutral $Fc(MeOH)_2$ probe (compare curves (6) and (5) in Fig. 4B) because it did not induce any electrostatic effect. This demonstrates that the charge selectivity of the protonated Amino-AT material remained effective in the amino-mesoporous silica composite film, enabling fast transport/accumulation of anions (and neutral molecules) while preventing the uptake of the positively-charged species. This is thus promising for the use of GCE/APTES-Amino-AT-Silica as an electrochemical sensor for DCF.

3.3. Factors affecting diclofenac preconcentration and detection

3.3.1. Influence of the amount of Amino-AT on the electrode

The accumulation capacity of the composite film on the GCE is expected to depend on the amount of Amino-AT in the dispersion used to modify the electrode surface. The anodic peak intensity was larger when increasing the amount of Amino-AT, and reaches a maximum value

corresponding to 5 mg of Amino-AT (Fig. 5). Beyond this content, the current intensity decreases, the too thick films starting to act as a barrier to the detection of the analyte. 5 mg is then taken as the optimal amount of Amino-AT in the dispersion.

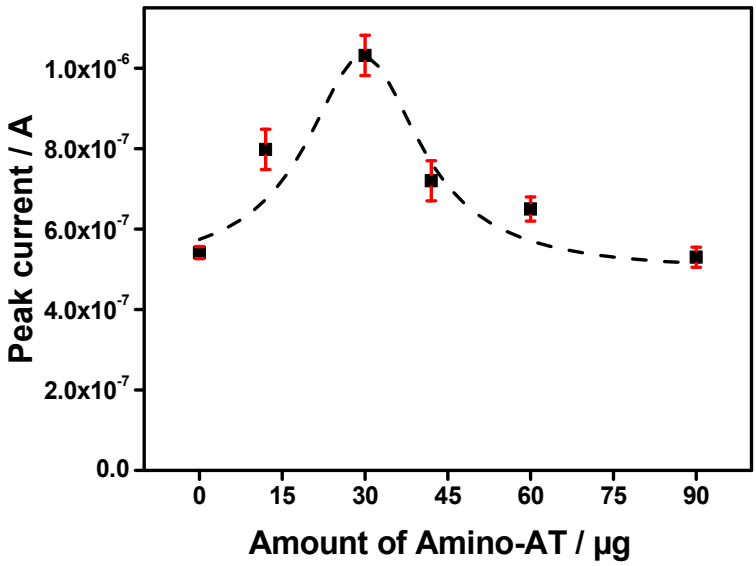

Fig. 5. Effect of the amount of Amino-AT (in µg) on the SWV peak current of 5 µM DCF on GCE/Amino-AT. Accumulation time: 2 min in 0.1 M phosphate buffer pH 5.7. Experiments were performed in triplicate.

3.3.2. Effect of the presence of silica on the Amino-AT modified electrode response

Prior to the exploitation of the amino-attapulgite/mesoporous silica composite film as sensing material, the difference in its electrochemical response to DCF relative to that of silica-free GCE/Amino-AT should be examined. The results shown in Fig. 6 indicate only little sensitivity difference between GCE/Amino-AT-silica and GCE/Amino-AT electrodes. Actually, the electrode modified with the Amino-AT-silica composite film was protonated because the extraction of surfactant from the mesoporous silica was made in acidic medium (EtOH/HCl 1:1). So, the most realistic comparison has to be made with respect to protonated GCE/Amino-AT (which contributes to facilitate the accumulation of negatively charged DCF); again, little difference in peak current intensity for DCF was observed (only a signal slightly lower in the presence of silica), confirming that the mesoporous silica binder does not affect significantly the accumulation ability of the amino-attapulgite material. Note that a small anodic shift in peak potentials is noticeable for protonated GCE/Amino-AT and GCE/APTES-Amino-AT-Silica (also protonated as a result of surfactant extraction in acidic

ethanolic solution) electrodes, which might be due to some local pH increase around Amino-AT particles (in agreement with peak potentials variations reported on Fig. 2A). The potential shift is even slightly more marked in the presence of the mesoporous silica binder, suggesting possible lower electron transfer rates for DCF oxidation (that might result from electrostatic repulsions originating from the silica surface, which is negatively charged at pH > 4 [70]).

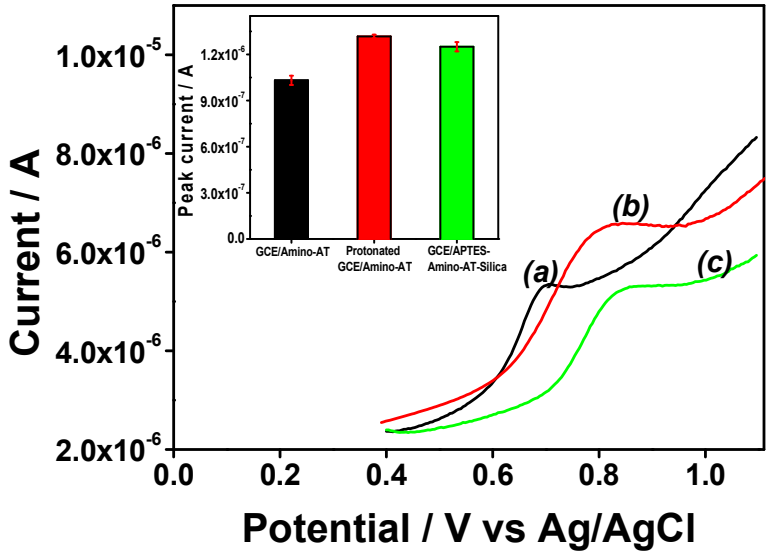

Fig. 6. SWV curves obtained on (a) GCE/Amino-AT (black), (b) protonated GCE/Amino-AT (in a separate solution of 0.1 M HCl and washing with water prior to use) (red) and (c) GCE/APTES-Amino-AT-Silica (green). Detection was performed in triplicate in in 0.1 M phosphate buffer pH 5.7 containing 5 µM DCF. Accumulation time: 2 min. The inset shows peak current values measured after background subtraction.

3.3.3. Influence of accumulation time

Figure 7 shows the dependence of SWV peak currents on the accumulation time for the analysis of 5 µM DCF at GCE/Amino-AT and GCE/APTES-Amino-AT-Silica electrodes. On both electrodes, the response was very fast, being at about 50% of its maximal value before applying any preconcentration step and then increasing gradually and almost linearly with the accumulation time up to 3-4 min, to reach a plateau when preconcentration was performed for longer periods. The plateau indicates that a saturation of binding sites and reaching a rather fast adsorptive equilibrium is probably imputable to low resistance to mass transport in such highly porous film electrodes. The threshold value of 3-4 min accumulation of DCF was thus used afterwards.

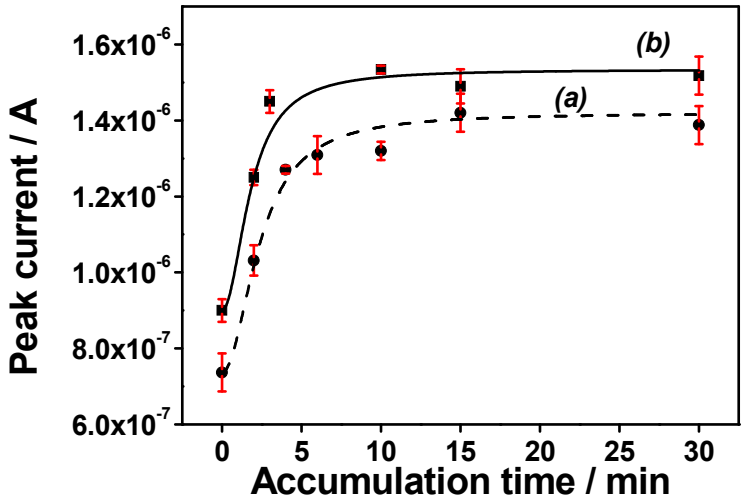

Fig. 7. Influence of the accumulation time on SWV peak currents recorded in triplicate for the detection of 5 µM DCF (in 0.1 M phosphate buffer pH 5.7) using (a) GCE/Amino-AT and (b) GCE/APTES-Amino-AT-Silica electrode.

3.3.4. Calibration

The effect of concentration of diclofenac on peak current was studied at optimized conditions and the calibration curve was found to be linear in the concentration range from 0.3 to 10 µM on GCE/APTES-Amino-AT-silica (Fig. 8). The measurements were performed in triplicate and an average value of the current is reported, with error bars included in the inset. The linearity of peak current (Ip) *vs.* concentration was maintained up to 20 µM (with a sensitivity of 0.125 A M^{-1}, and correlation coefficient of 0.998) and then tended to level off when increasing DCF concentration up to 50 µM (see Fig. S5 in Supplementary Material). The sensitivity was almost the same (yet lower by ca. 10%) for GCE/Amino-AT electrode (0.111 A M^{-1}), in agreement with the above observations (Fig. 6). The detection limit D_L, is based on an analytical signal corresponding to the minimum detectable peak intensity. D_L can be defined as the analyte concentration yielding such smallest detectable signal and is calculated from the standard deviation of the blank (σ) and the slope of the calibration line (*b*), according to the equation $D_L = 3\sigma/b$ [71]. In this work, D_L values were estimated to be 0.204 µM on GCE/Amino-AT and 0.053 µM on GCE/APTES-Amino-AT-silica, on the basis of a signal to noise ratio of 3. Relative standard deviations (RSD) of 5.68 % and 5.62 % for parallel detections of 5 µM DCF using six distinct electrodes were obtained for GCE/Amino-AT and GCE/APTES-Amino-AT-Silica, respectively, indicating a good reproducibility and repeatability for both modified electrodes. A definite advantage of the GCE/APTES-Amino-

AT-Silica electrode is its better mechanical stability and thus repeatable SWV response upon successive measurements (Fig. 9), thanks to the physical entrapment of clay particles in the silica matrix avoiding their leaching in solution during the cleaning step of the electrode.

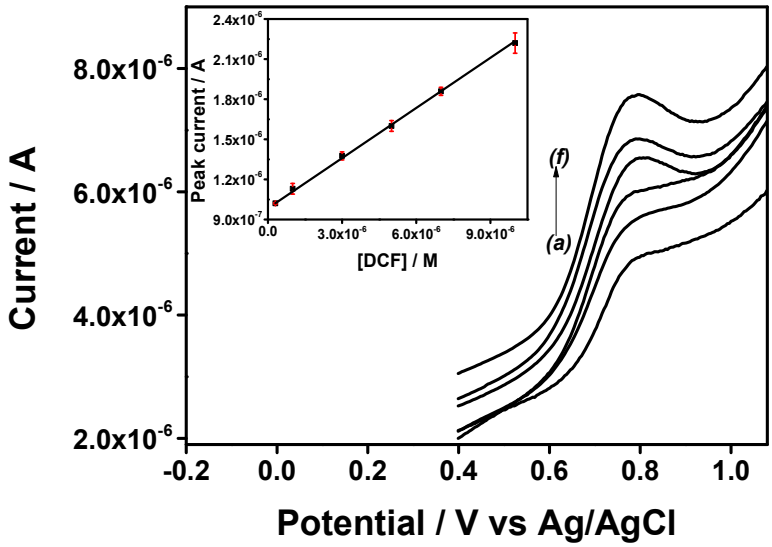

Fig. 8. Square-wave voltammograms recorded for DCF in phosphate buffer pH 5.7, in the 0.3 to 10 µM concentration range, using GCE/APTES-Amino-AT-Silica electrode. Inset: corresponding calibration curve obtained from SWV curves recorded in triplicates. Accumulation time: 3 min.

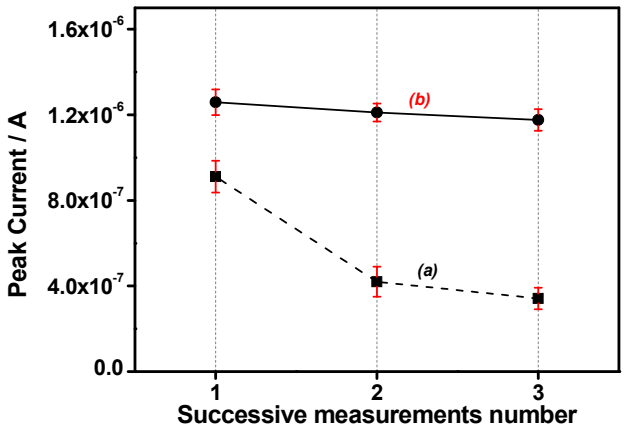

Fig. 9. SWV responses recorded in triplicate with (a) GCE/Amino-AT and (b) GCE/APTES-Amino-AT-Silica to successive preconcentration/detection of 5 µM DCF in phosphate buffer pH 5.7 after 2 min accumulation. A step of cleaning the surface of the modified electrode between each successive measurement has been applied under stirring for 15 min in (a) 0.1 M HCl and (b) ethanol solution (to remove the adsorbed DCF oxidation products).

The performance of the method proposed herein is comparable, and even better than some data already reported on the quantification of DCF using other modified electrodes [23,60-62,72-75], as shown in Table 1.

Table 1: Comparison of the performance of some DCF sensors based on modified electrodes.

Modified electrode configuration	Linear range (µM)	Detection limit (µM)	Sensitivity ($\mu A.\mu M^{-1}$)	Technique	Reference
IL/CNTPE	0.3 - 750	0.09	0.0999	SWV	[7]
MWCNTs-G/Ag electrode	0.14 - 6.29	0.047	0.0008	SWV	[23]
MWCNTs/$Cu(OH)_2$/IL	0.18 - 119	0.04	0.0147	DPV	[60]
EPPG	0.010 - 1	0.0062	69	SWV	[61]
SWCNT/EPPGE	0.001 - 0.5 0.025 - 1.5	0.00082 0.022.5	224.0 51.0	SWV	[62]
TCPE	10 - 140	3.28	0.1905	DPV	[72]
NHMN electrode	196 - 2650	31.7	0.0012	A	[73]
GO-COOH/GCE	1.2-400	0.09	0.532	LSV	[74]
AuNPs/MWCNTs/GCE	0.03-200	0.02	0.9329	SWV	[75]
GCE/Amino-AT	0.3-20	0.204	0.139	SWV	This work
GCE/APTES-Amino-AT-Silica	0.3-10	0.053	0.125	SWV	This work

SWV: Square Wave Voltammetry, DPV: Differential Pulse Voltammetry, A: amperometry LSV: Linear Sweep Voltammetry

3.4. Analytical applications – real samples analysis

In order to demonstrate the ability of the modified electrodes for the determination of DCF in real samples, a pharmaceutical product and three water samples (Tap water, mineral water and SB water) were examined. The proposed method was first applied to the determination of DCF sodium in DCF gastro-resistant coated tablet (Voltaren®). The results are reported in Table 2. In this experiment, the concentration of diclofenac sodium was calculated using standard additions method. As shown, recovery values close to 100% were obtained with respect to the supplier specifications, indicating good confidence level of the modified electrodes. Tap water and mineral water were stored in a refrigerator immediately after collection (from the LCPME laboratory and the market, respectively). The natural water sample from the Strengbach Watershed (a granitic watershed located in NE of France, in the Vosges Mountains) referred as SB water was collected, filtered using a 0.45 µm filter and stored in a refrigerator. All water samples were conditioned with phosphate buffer (pH 5.7). The solutions were transferred into the voltammetric cell to be analyzed without any further treatment. As shown in Table 3, a high recovery was obtained for all water samples spiked with DCF, suggesting that the two sensors are promising for practical detection of diclofenac.

Table 2. Determination of DCF in pharmaceutical preparations using GCE/Amino-AT and GCE/APTES-Amino-AT-Silica.

Electrode	Sample	Stated content	Detected content	Recovery (%)
GCE/Amino-AT	Voltaren®	25 mg	24.2 mg	96.8 (n=6)
GCE/APTES-Amino-AT-Silica			25.9 mg	103.5 (n=5)

Table 3. Determination of DCF in Water samples using GCE/Amino-AT and GCE/APTES-Amino-AT-Silica.

Electrode	Type of water[(a)]	Added (µM)	Found[(b)] (µM)	RSD[(c)]	Recovery (%)
GCE/Amino-AT	Tap water	3.00	2.81	1.69 %	93.7
	Mineral water	3.00	3.10	1.42 %	104
	SB water	3.00	3.21	4.01 %	107
GCE/APTES-Amino-AT-Silica	Tap water	0.30	0.29	3.40 %	95.6
	Mineral water	0.30	0.33	3.73 %	110
	SB water	0.30	0.35	2.51 %	117

(a) *All sample water samples were collected from Nancy, France.*

(b) *Mean of three measurements*

(c) *Relative standard deviation for n = 3.*

4. Conclusion

Two new modified electrodes (GCE/Amino-AT and GCE/APTES-Amino-AT-Silica) have been characterized using cyclic voltammetry, SEM and EDX analyses, and then applied to the sensitive detection of diclofenac. The amino-AT-mesoporous silica composite films generated on glassy carbon electrode pretreated by electrografting of APTES was more mechanically stable after use than the Amino-AT modified GCE. Both were highly porous, exhibiting good accumulation ability for negatively charged species, owing to the positive charges present on the organoclay (protonated amino groups). Under the optimized conditions, the peak currents recorded by SWV were linear to DCF concentrations in the 0.3 to 20 µM range, with detection limits of 0.204 µM and 0.053 µM, respectively for GCE/Amino-AT and GCE/APTES-Amino-AT-Silica electrodes. The proposed sensors were successfully applied to the determination of DCF in pharmaceutical and water samples.

Acknowledgments

The authors are grateful to the Agence Universitaire de la Francophonie (France) for a support through the programme *Soutien aux Equipes de Recherche*. Financial support from The World Academy of Sciences for the Advancement of Science in Developing Countries (TWAS grant no. 12-117 RG/CHE/AF/AC-G awarded to I.K. Tonle) is also acknowledged. Dr Grégoire Herzog (Université de Lorraine, France) is thanked for facilitation in SEM and EDX analyses.

References

[1] L. Campanella, G. Di Persio, M. Pintore, D. Tonnina, N. Caretto, E. Martini, D. Lelo, Determination of nonsteroidal anti-inflammatory drugs (NSAIDs) in milk and fresh cheese based on the inhibition of cyclooxygenase, Food Technol. Biotechnol. 47 (2009) 172–177.

[2] X. Zhao, Y. Hou, H. Liu, Z. Qiang, J. Qu, Electro-oxidation of diclofenac at boron doped diamond: Kinetics and mechanism, Electrochim. Acta 54 (2009) 4172–4179.

[3] L.H.M.L.M. Santos, A.N. Araújo, A. Fachini, A. Pena, C. Delerue-Matos, M.C.B.S.M. Montenegro, Ecotoxicological aspects related to the presence of pharmaceuticals in the aquatic environment, J. Hazard. Mater. 175 (2010) 45–95.

[4] A.C. Collier, Pharmaceutical contaminants in potable water: potential concerns for pregnant women and children, Eco. Health 4 (2007) 164–171.

[5] M.S.M. Quintino, K. Araki, H.E. Toma, L. Angnes, Amperometric quantification of sodium metabisulfite in pharmaceutical formulations utilizing tetraruthenated porphyrin film modified electrodes and batch injection analysis, Talanta 68 (2006) 1281–1286.

[6] T. Iliescu, M. Baia, V. Miclăuş, A Raman spectroscopic study of the diclofenac sodium-betacyclodextrin interaction, Eur. J. Pharm. Sci. 22 (2004) 487–495.

[7] M. Goodarzian, M.A. Khalilzade, F. Karimi, V.K. Gupta, M. Keyvanfard, H. Bagheri, M. Fouladgar, Square wave voltammetric determination of diclofenac in liquid phase using a novel ionic liquid multiwall carbon nanotubes paste electrode, J. Mol. Liq. 197 (2014) 114–119.

[8] A. Azzouz, B. Jurado-Sanchez, B. Souhail, E. Ballesteros, Simultaneous Determination of 20 Pharmacologically Active Substances in Cow's Milk, Goat's Milk, and Human Breast Milk by Gas Chromatography Mass Spectrometry, J. Agric. Food Chem. 59 (2011) 5125–5132.

[9] B. Yilmaz, U. Ciltas, Determination of diclofenac in pharmaceutical preparations by voltammetry and gas chromatography methods, J. Pharm. Anal. 5 (2015) 153–160.

[10] P.C. Damiani, M. Bearzotti, M.A. Cabezon, A.C. Olivieri, Spectrofluorometric determination of diclofenac in tablets and ointments, J. Pharm. Biomed. Anal. 20 (1999) 587–590.

[11] I. Kramancheva, I. Dobrev, L. Brakalov, A. Andreeva, Spectrophotometric determination of diclofenac sodium in gel-ointment, Anal. Lett. 30 (1997) 2235–2249.

[12] M.S. Garcia, M.I. Albero, C. Sanchez-Pedreno, J. Molina, Flow-injection spectrophotometric determination of diclofenac sodium in pharmaceuticals and urine samples, J. Pharm. Biomed. Anal. 17 (1998) 267–273.

[13] S.C. Liu, T.H. Tsai, Determination of diclofenac in rat bile and its interaction with cyclosporin A using on-line microdialysis coupled to liquid chromatography, J. Chromatogr. B 796 (2002) 351–356.

[14] E.F. Elkady, Simultaneous determination of diclofenac potassium and methocarbamol in ternary mixture with guaifenesin by reversed phase liquid chromatography, Talanta 82 (2010) 1604–1607.

[15] L. Kaphalia, B.S. Kaphalia, S. Kumar, M.F. Kanz, M. Treinen-Moslen, Efficient high performance liquid chromatograph/ultraviolet method for determination of diclofenac and 4′-hydroxydiclofenac in rat serum, J. Chromatogr. B 830 (2006) 231–237.

[16] H.S. Lee, C.K. Jeong, S.J. Choi, S.B. Kim, M.H. Lee, G. Ko, D.H. Sohn, Simultaneous determination of aceclofenac and diclofenac in human plasma by narrowbore HPLC using column-switching, J. Pharm. Biomed. Anal. 23 (2000) 775–781.

[17] C.P. Sastry, T. Prasad, M.V. Suryamarayana, Spectrophotometric method for determination of diclofenac sodium in bulk samples and pharmaceutical preparations, Analyst 114 (1989) 513–516.

[18] C. Arcelloni, R. Lanzi, S. Pedercini, G. Molteni, I. Fermo, A. Pontiroli, R. Paroni, High-performance liquid chromatographic determination of diclofenac in human plasma after solid-phase extraction, J. Chromatogr. B 763 (2001) 195–200.

[19] L. González, G. Yuln, M.G. Volonté, Determination of cyanocobalamin, betamethasone, and diclofenac sodium in pharmaceutical formulations, by high performance liquid chromatography, J. Pharm. Biomed. Anal. 20 (1999) 487–492.

[20] A.S. Birajdar, S. Meyyanathan, B. Suresh, A RP-HPLC method for determiınatıon of diclofenac with rabeprazole in solid dosage form, Pharm. Sci. Monit. 2 (2011) 171–178.

[21] X. Yang, F. Wang, S. Hu, Enhanced oxidation of diclofenac sodium at a nanostructured electrochemical sensing film constructed by multi-wall carbon nanotubes–surfactant composite, Mater. Sci. Eng. C 28 (2008) 188–194.

[22] F. Manea, M. Ihos, A. Remes, G. Burtica, J. Schoonman, Electrochemical determination of diclofenac sodium in aqueous solution on Cu-doped zeolite-expanded graphite-epoxy electrode, Electroanalysis 22 (2010) 2058–2063.

[23] A. Bayandori Moghaddam, A. Mohammadi, M. Fathabadi, Application of carbon nanotube-graphite mixture for the determination of diclofenac sodium in pharmaceutical and biological samples, Pharmaceut. Anal. Acta 3 (2012) 1–6.

[24] J. Vahedi, H. Karimi-Maleh, M. Baghayeri, A.L. Sanati, M.A. Khalilzadeh, M. Bahrami, A fast and sensitive nanosensor based on MgO nanoparticle room-temperature ionic liquid carbon paste electrode for determination of methyldopa in pharmaceutical and patient human urine samples, Ionics 19 (2013) 1907–1914.

[25] S. Thiagarajan, M. Rajkumar, S.M. Chen, Nano TiO_2-PEDOT film for the simultaneous detection of ascorbic acid and diclofenac, Int. J. Electrochem. Sci. 7 (2012) 2109–2122.

[26] Y. Akbarian, M. S.-Nooshabadi, H. K.-Maleh, Fabrication of a new electrocatalytic sensor for determination of diclofenac, morphine and mefenamic acid using synergic effect of NiO-SWCNT and 2, 4-dimethyl-N/-[1-(2, 3-dihydroxyphenyl)methylidene]aniline, Sens. Actuators B 273 (2018) 228–233.

[27] H. Chen, Z. Zhang, D. Cai, S. Zhang, B. Zhang, J. Tang, Z. Wu, Attapulgite with poly(methylene blue) composite film electrocatalytic determination of ascorbic acid, Solid State Sciences 14 (2012) 362–366.

[28] A. Maghear, C. Cristea, A. Marian, I.O. Marian, R. Săndulescu, A novel biosensor for acetaminophen detection with romanian clays and conductive polymeric films, Farmacia 61 (2013) 1–11.

[29] M. Park, I.K. Shim, E.Y. Jung, J.H. Choy, Modification of external surface of laponite by silane grafting, J. Phys. Chem. Solids 65 (2004) 499–501.

[30] F. Piscitelli, P. Posocco, R. Toth, M. Fermeglia, S. Pricl, G. Mensitieri, M. Lavorgna, Sodium montmorillonite silylation: unexpected effect of the aminosilane chain length, J. Colloid Interface Sci. 351 (2010) 108–115.

[31] G. Lagaly, M. Ogawa, I. Dekany, Clay minerals organic interactions, in: F. Bergaya, G. Lagaly (Eds.), Handbook of Clay Science. Developments in Clay Science, vol. A, 2nd edition, Elsevier, 2013, 435–505.

[32] M. Pal, V. Ganesan, Effect of gold nanoparticles on the electrocatalytic reduction of oxygen by silica encapsulated cobalt phthalocyanine, J. Electroanal. Chem. 672 (2012) 7-11.

[33] D. Tarn, C. E. Ashley, M. Xue, E. C. Carnes, J. I. Zink, C. J. Brinker, Mesoporous silica nanoparticle nanocarriers: biofunctionality and biocompatibility, Acc. Chem. Res. 46 (2013) 792–801.

[34] R. Gupta, V. Ganesan, Gold nanoparticles impregnated mesoporous silica spheres for simultaneous and selective determination of uric acid and ascorbic acid, Sens. Actuators B 219 (2015) 139–145.

[35] A. Walcarius, L. Mercier, Mesoporous organosilica adsorbents: nanoengineered materials for removal of organic and inorganic pollutants, J. Mater. Chem. 20 (2010) 4478–4511.

[36] L. Gibson, Mesosilica materials and organic pollutant adsorption: part B removal from aqueous solutions, Chem. Soc. Rev. 43 (2014) 5173–5182.

[37] V. Urbanova, A. Walcarius, Vertically-aligned mesoporous silica films, Z. Anorg. Allg. Chem. 640 (2014) 537–546.

[38] P. Innocenzi, L. Malfatti, T. Kidchob, P. Falcaro, Order-disorder in self-assembled mesostructured silica films: A concepts review, Chem. Mater. 21 (2009) 2555–2564.

[39] C. Sanchez, C. Boissiere, D. Grosso, C. Laberty, L. Nicole, Design, synthesis, and properties of inorganic and hybrid thin films having periodically organized nanoporosity, Chem. Mater. 20 (2008) 682–737.

[40] A. Walcarius, Chem. Soc. Rev. 42 (2013) 4098–4140.

[41] A. Walcarius, E. Sibottier, M. Etienne, J. Ghanbaja, Electrochemically assisted self-assembly of mesoporous silica thin films, Nat. Mater. 6 (2007) 602–608.

[42] A. Goux, M. Etienne, E. Aubert, C. Lecomte, J. Ghanbaja, A. Walcarius, Oriented mesoporous silica films obtained by electro-assisted self-assembly (EASA), Chem. Mater. 21 (2009) 731–741.

[43] R. Shacham, D. Avnir, D. Mandler, Electrodeposition of methylated sol–gel films on conducting surfaces, Adv. Mater. 11 (1999) 384–388.

[44] P.N. Deepa, M. Kanungo, G. Claycomb, P.M.A. Sherwood, M.M. Collinson, Electrochemically deposited sol-gel-derived silicate films as a viable alternative in thin-film design, Anal. Chem. 75 (2003) 5399–5405.

[45] M.M. Collinson, Electrochemistry: an important tool to study and create new sol–gel-derived materials, Acc. Chem. Res. 40 (2007) 777–783.

[46] M. Etienne, A. Goux, E. Sibottier, A. Walcarius, Oriented mesoporous organosilica films on electrode: a new class of nanomaterials for sensing, J. Nanosci. Nanotechnol. 9 (2009) 2398–2406.

[47] O. Nadzhafova, M. Etienne, A. Walcarius, Direct electrochemistry of hemoglobin and glucose oxidase in electrodeposited sol–gel silica thin films on glassy carbon, Electrochem. Commun. 9 (2007) 1189–1195.

[48] Z. Wang, M. Etienne, G.-W. Kohring, Y. Bon Saint Côme, A. Kuhn, A. Walcarius, Electrochemically assisted deposition of sol–gel bio-composite with co-immobilized dehydrogenase and diaphorase, Electrochim. Acta 56 (2011) 9032–9040.

[49] A. Maghear, M. Etienne, M. Tertis¸ R. Sandulescu, A. Walcarius, Clay-mesoporous silica composite films generated by electro-assisted self-assembly, Electrochim. Acta 112 (2013) 333–341.

[50] T. Nasir, L. Zhang, N. Vilà, G. Herzog, A. Walcarius, Electrografting of 3-aminopropyltriethoxysilane on a glassy carbon electrode for the improved adhesion of vertically oriented mesoporous silica thin films, Langmuir 32 (2016) 4323–4332.

[51] A. Xue, S. Zhou, Y. Zhao, X. Lu, P. Han, Effective NH_2-grafting on attapulgite surfaces for adsorption of reactive dyes, J. Hazard. Mater. 194 (2011) 7–14.

[52] B. Gu, H. Zhong, L. Zhang, Z. Cheng, Y. Wang, X. Li, J. Xu, C. Yao, Attapulgite clay combined with Tris(2, 2'bipyridyl)ruthenium(II) for the enhancement of the electrogenerated chemiluminescence sensing, Int. J. Electrochem. Sci. 7 (2012) 6202–6213.

[53] L.R. Frost, V. Vagvolgyi, M.L. Daniel, S.C. Pinto, J. Kristof, E. Horvath, Dynamic and controlled rate thermal analysis of attapulgite, J. Therm. Anal. Calorim. 92 (2008) 589–594.

[54] J. Duan, S. Shao, L. Jiang, Y. Li, P. Jing, B. Liu, Nano-attapulgite functionalization by silane modification for preparation of covalently-integrated epoxy/TMPTMA nanocomposites, Iran. Polym. J. 20 (2011) 855–872.

[55] L. Xuefeng, Y. Xu, T. Xin, W. Lin, S. Yuebing, L. Dasong, S. Yang, Q. Xu, W. Qian, Heavy metal adsorbents mercapto and amino functionalized palygorskite: preparation and characterization, Colloids Surf. A 426 (2013) 98–105.

[56] S.L.Z. Jiokeng, L.M. Dongmo, E. Ymele, E. Ngameni, I.K. Tonle, Sensitive stripping voltammetry detection of Pb(II) at a glassy carbon electrode modifed with an aminofunctionalized attapulgite. Sens. Actuators B 242 (2017) 1027–1034.

[57] F.M.M. Tchieno, L.S. Guenang, E. Ymele, E. Ngameni, I.K. Tonle. Electroanalytical application of amine-grafted attapulgite to the sensitive quantification of the bioactive compound mangiferin, Electroanalysis 29 (2017) 529–537.

[58] A. Adenier, M.M. Chehimi, I. Gallardo, J. Pinson, N. Vilà, Electrochemical oxidation of aliphatic amines and their attachment to carbon and metal surfaces, Langmuir 20 (2004) 8243–8253.

[59] G. Newcombe, R. Hayesb, M. Drikas, Granular activated carbon: importance of surface properties in the adsorption of naturally occurring organics, Colloids Surf. A 78 (1993) 65–71.

[60] M. Arvand, T.M. Gholizadeh, M. A. Zanjanchi, MWCNTs/$Cu(OH)_2$ nanoparticles/IL nanocomposite modified glassy carbon electrode as a voltammetric sensor for determination of the non-steroidal anti-inflammatory drug diclofenac, Mater. Sci. Eng. C 32 (2012) 1682–1689.

[61] R. N. Goyal, S. Chatterjee, B. Agrawal, Electrochemical investigations of diclofenac at edge plane pyrolytic graphite electrode and its determination in human urine, Sens. Actuators B 145 (2010) 743–748.

[62] R.N. Goyal, S. Chatterjee, A.R.S. Rana, The effect of modifying an edge-plane pyrolytic graphite electrode with single-wall carbon nanotubes on its use for sensing diclofenac, Carbon 48 (2010) 4136–4144.

[63] C. Ràfols, M. Rosés, E. Bosch, A comparison between different approaches to estimate the aqueous pK_a values of several non-steroidal anti-inflammatory drugs, Anal. Chim. Acta 338 (1997) 127–134.

[64] Y. Chi, Y. Chen, X. Liu, Z. Guo, J. Xiao, J. Xu, W. Zhao, Impact of environmental conditions on the sorption behavior of Pb(II) onto attapulgite, J. Radioanal. Nucl. Chem. 295 (2013) 1589–1596.

[65] S.M. Macha, A. Fitch, Clays as architectural units at modified-electrodes, Microchim. Acta 128 (1998) 1–18.

[66] M. Etienne, S. Sallard, M. Schröder, Y. Guillemin, S. Mascotto, B.M. Smarsly, A. Walcarius, Electrochemical generation of thin silica films with hierarchical porosity, Chem. Mater. 22 (2010) 3426–3432.

[67] C.J. Brinker, W. Gong, Y. Guo, H. Soyez, B. Dunn, M.H. Huang, J.I. Zink, Continuous formation of supported cubic and hexagonal mesoporous films by sol–gel dip coating, Nature 389 (1997) 364–368.

[68] M. Etienne, A. Quach, D. Grosso, L. Nicole, C. Sanchez, A. Walcarius, Molecular transport into mesostructured silica thin films: electrochemical monitoring and comparison between *P*6*m*, $P6_3/mmc$, and *Pm*3*n* structures, Chem. Mater. 19 (2007) 844–856.

[69] N. Vilà, E. André, R. Ciganda, J. Ruiz, D. Astruc, A. Walcarius, Molecular sieving with vertically-aligned mesoporous silica films and electronic wiring through isolating nanochannels, Chem. Mater. 28 (2016) 2511–2514.

[70] T. Nasir, G. Herzog, M. Hebrant, C. Despas, L. Liu, A. Walcarius, Mesoporous silica thin films for improved electrochemical detection of paraquat, ACS Sens. 3 (2018) 484–493.

[71] M.M. Ghoneim, A.M. Hassanein, E. Hammam, A.M. Beltagi, Simultaneous determination of Cd, Pb Cu, Sb, Bi, Se, Zn, Mn, Ni, Co and Fe in water samples by differential pulse stripping voltammetry at a hanging mercury drop electrode, Fresenius J. Anal. Chem. 367 (2000) 378–383.

[72] B.K. Chethana, S. Basavanna, Y. Arthoba Naik, Voltammetric determination of diclofenac sodium using tyrosine- modified carbon paste electrode, Ind. Eng. Chem. Res. 51 (2012) 10287–10295.

[73] M. Hajjizadeh, A. Jabbari, H. Heli, A.A. Moosavi-Movahedi, S. Haghgoo, Electrocatalytic oxidation of some anti-inflammatory drugs on a nickel hydroxide-modified nickel electrode, Electrochim. Acta. 53 (2007) 1766–1774.

[74] C. Karuppiah, S. Cheemalapati, S.M. Chen, S. Palanisamy, Carboxyl-functionalized graphene oxide-modified electrode for the electrochemical determination of nonsteroidal anti-inflammatory drug diclofenac, Ionics 21 (2014) 231–238.

[75] A. Afkhami, A Bahiraei, T Madrakian, Gold nanoparticle/multi-walled carbon nanotube modified glassy carbon electrode as a sensitive voltammetric sensor for the determination of diclofenac sodium, Mater. Sci. Eng. C 59 (2016) 168–176.